Supporting Information for "Relationship Between Atmospheric Rivers and the Dry Season Extreme Precipitation in Central-Western Mexico"

H. A. Inda-Díaz[1], T. A. O'Brien[2,1]

[1]Climate and Ecosystem Sciences Division, Lawrence Berkeley National Laboratory, Berkeley, CA, USA

[2]Dept. of Earth and Atmospheric Sciences, Indiana University, Bloomington, IN, USA

Contents of this file

Corresponding author: T. A. O'Brien, Department of Earth and Atmospheric Sciences, Indiana University Bloomington. (obrienta@iu.edu)

February 7, 2023, 10:59pm

Text S1. Long-term means

In Figures S1 through S5, we present the times where each of the ERA-20C climatological means in the 1900-2010 for sea level ressure (SLP), geopotential height (Z), integrated water vapor (IWV), and integrated vapor transport (IVT).

Text S2. Additional plots for composites and their anomalies

In Figures S6 through S17, we present additional plots for the AR + Extreme preciption, AR + No Extreme Precipitation, and Extreme Precipitation + No AR composites. Left columns show IVT, IWV, SLP, Z at 850 and 500 hPa, vertical velocity (ω), and the direction of IVT. The right column shows the anomalies of each composite with respect to the climatological means.

Text S3. Time Correlation between AR and Extreme Precipitation Events

In Figures S18 through S25, we present the times where each of the composites is present at `Loc1` for the entire 1900-2010 period. We notice that AR detection (blue circle markers) are in general around the same dates that the extreme precipitation events (purple cross markers), in some cases before or after, but around each other. It is possible that an ARDTs tuned for tropical ARs would better detect ARs near CWM. Moreover, in future works, we could explore different reanalysis or precipitation data that, together with a tropical ARDT, could mean an even more significant correlation between extreme dry-season precipitation and ARs in CWM. The captions from S18 apply for Figures S19-S25.

Long-term Means

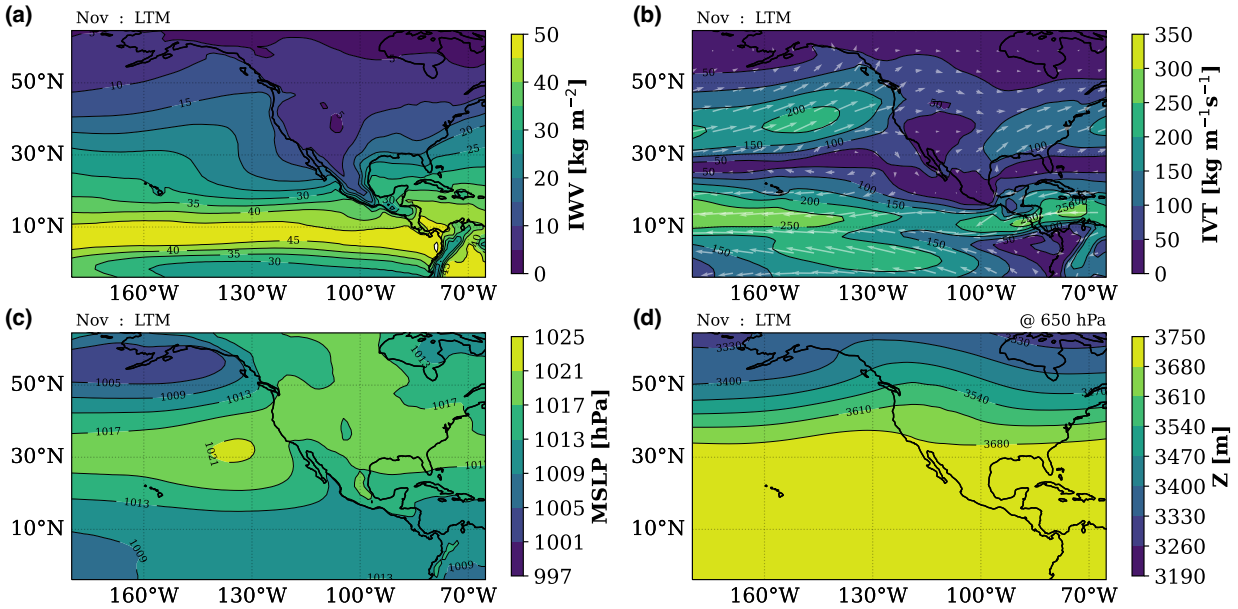

Figure S1. Long-term mean for 1900-2010. (a) Integrated water vapor (IWV), (b) integrated vapor transport (IVT), (c) mean sea level pressure (MSLP), (d) geopotential height at 650 hPa

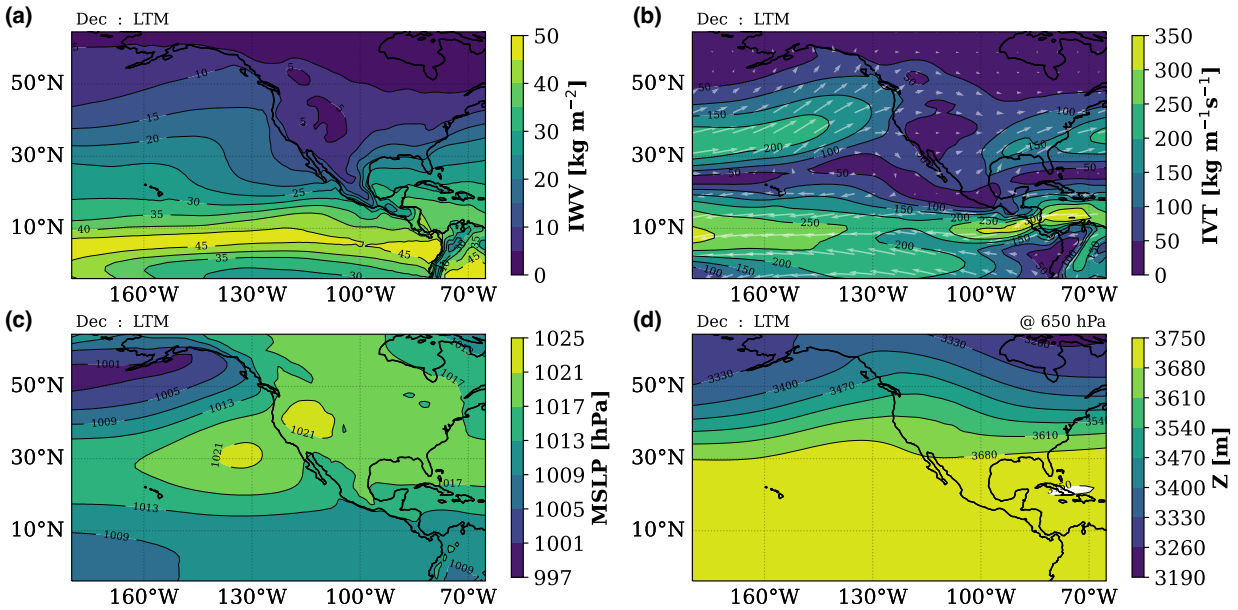

Figure S2. Long-term mean for 1900-2010. (a) Integrated water vapor (IWV), (b) integrated vapor transport (IVT), (c) mean sea level pressure (MSLP), (d) geopotential height at 650 hPa

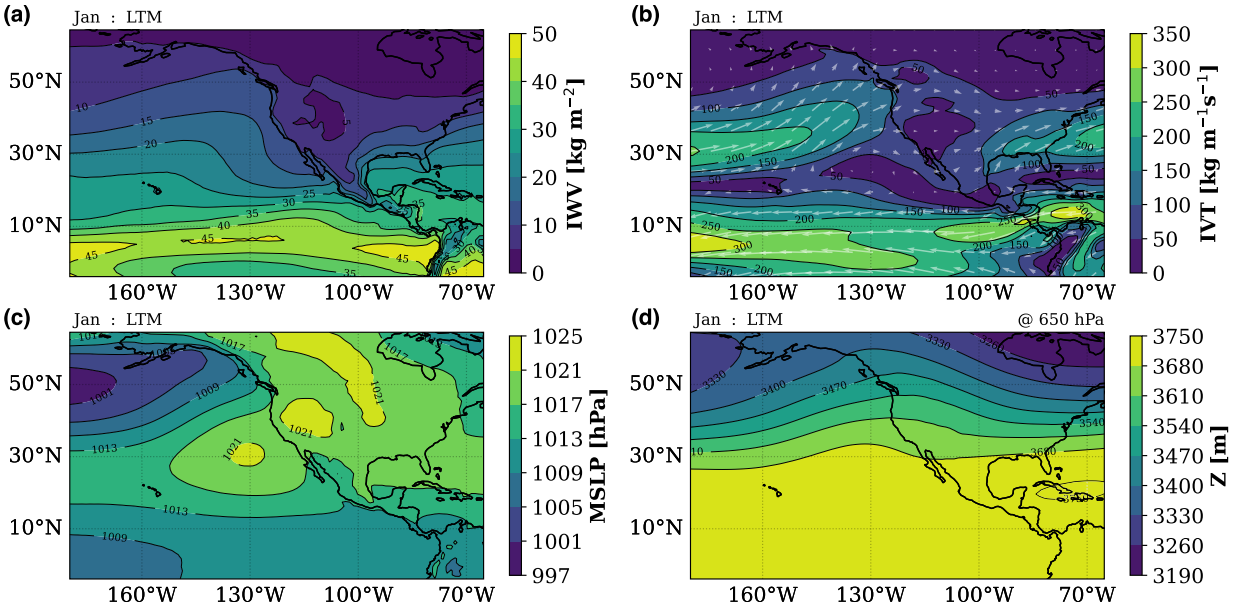

Figure S3. Long-term mean for 1900-2010. (a) Integrated water vapor (IWV), (b) integrated vapor transport (IVT), (c) mean sea level pressure (MSLP), (d) geopotential height at 650 hPa

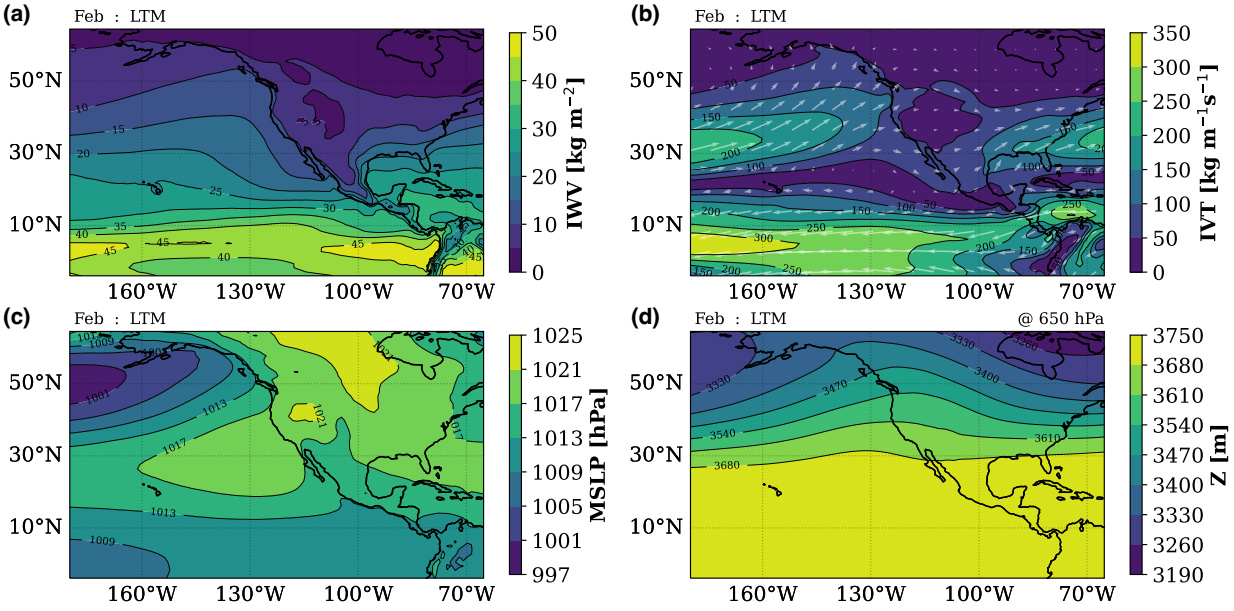

Figure S4. Long-term mean for 1900-2010. (a) Integrated water vapor (IWV), (b) integrated vapor transport (IVT), (c) mean sea level pressure (MSLP), (d) geopotential height at 650 hPa

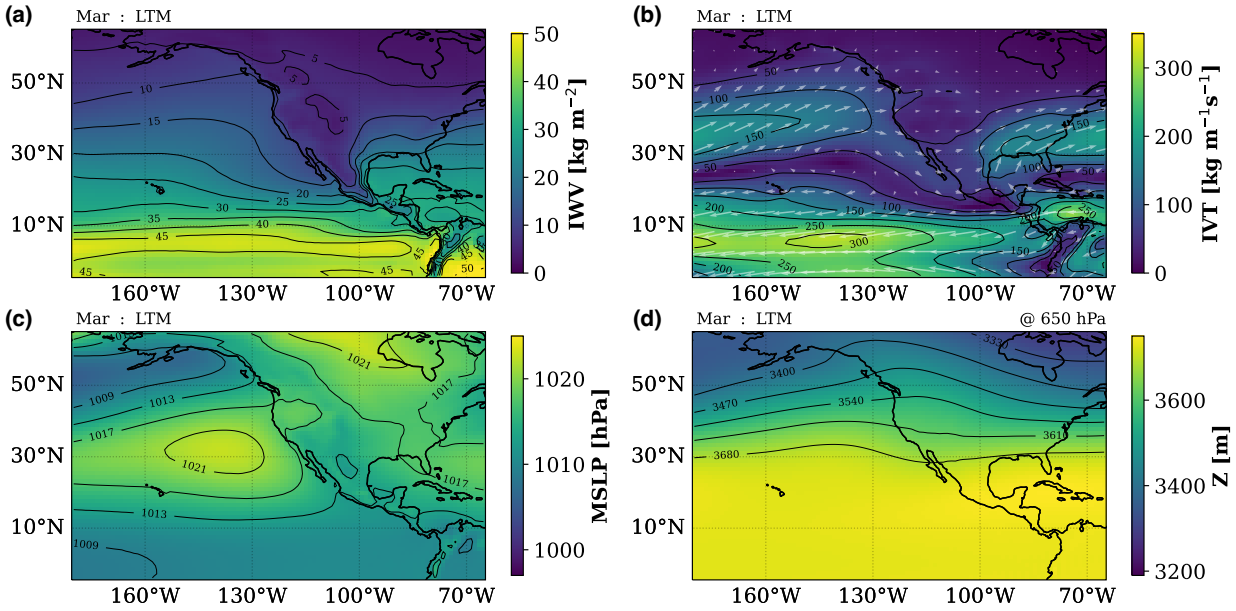

Figure S5. Long-term mean for 1900-2010. (a) Integrated water vapor (IWV), (b) integrated vapor transport (IVT), (c) mean sea level pressure (MSLP), (d) geopotential height at 650 hPa

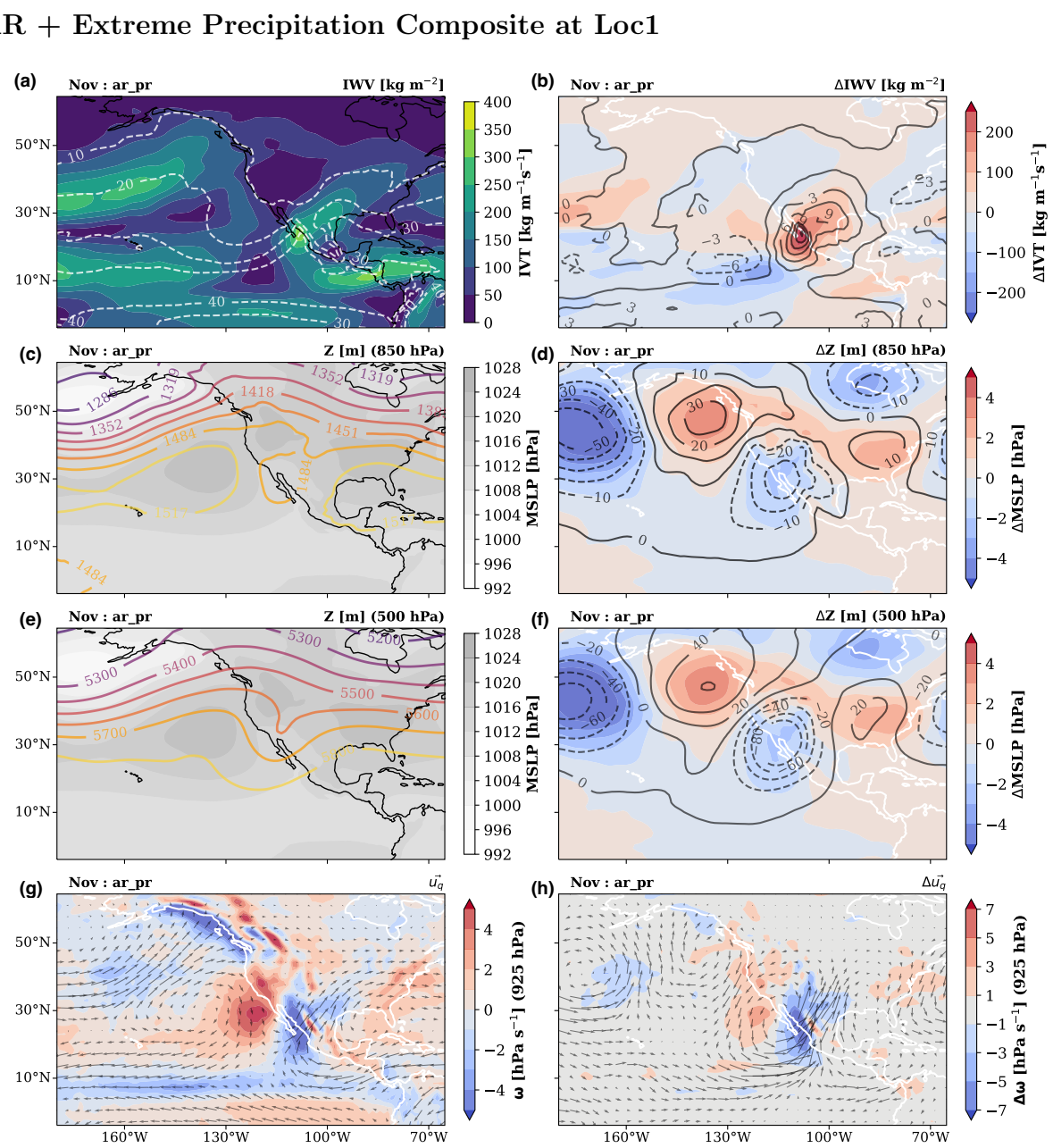

Figure S6. State of the atmosphere during AR landfalling and extreme precipitation at `Loc1` in November. Black contours variables are specified on the top-right of each plot. Left column: IWV, IVT, mean sea level pressure, geopotential height at 850 and 500 hPA, IVT direction (u_q), and ω at 650 hPa. Right column: anomalies with respect to the long-term mean for the same variables.

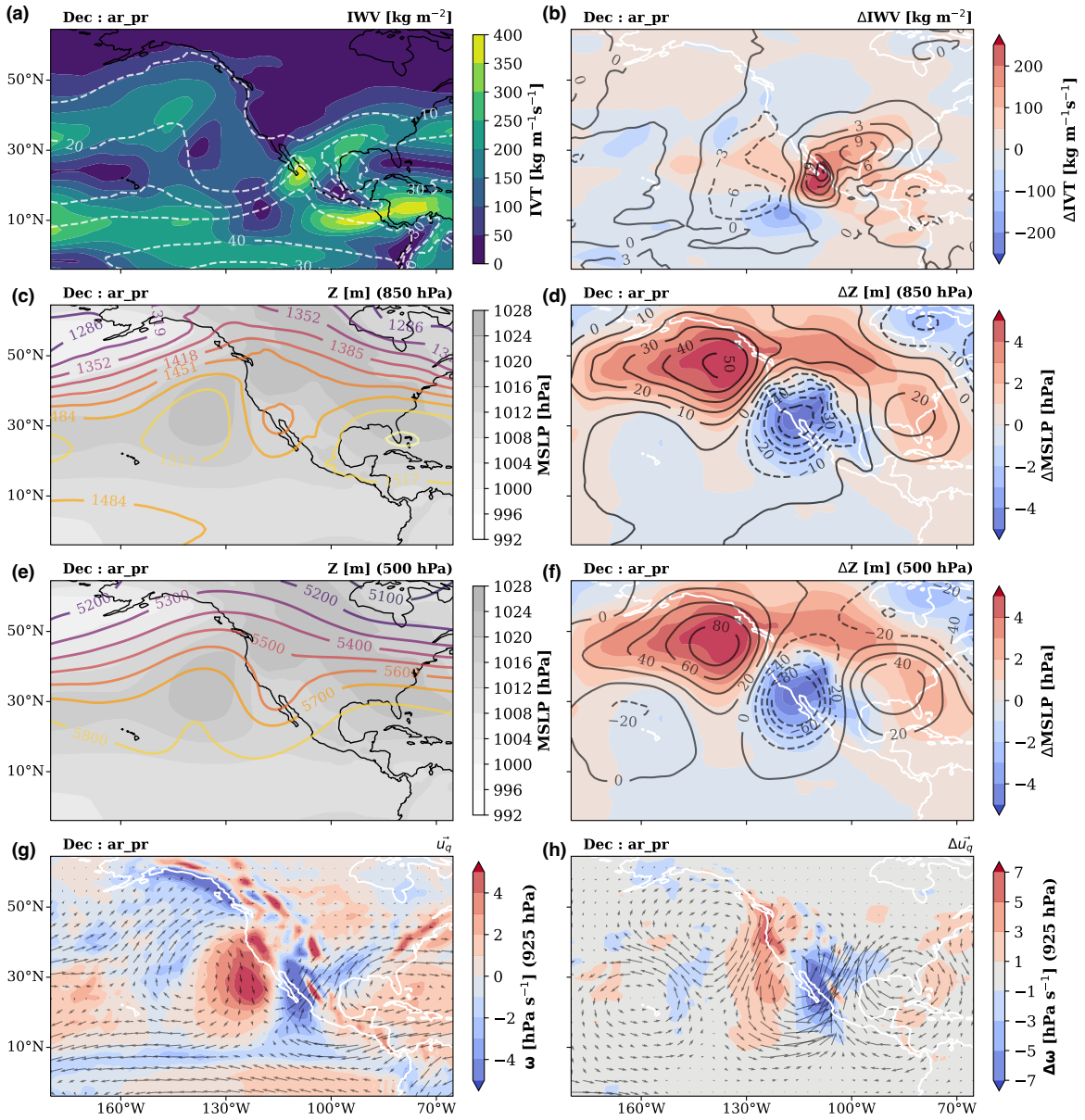

Figure S7. State of the atmosphere during AR landfalling and extreme precipitation at `Loc1` in December. Black contours variables are specified on the top-right of each plot. Left column: IWV, IVT, mean sea level pressure, geopotential height at 850 and 500 hPA, IVT direction (u_q), and ω at 650 hPa. Right column: anomalies with respect to the long-term mean for the same variables.

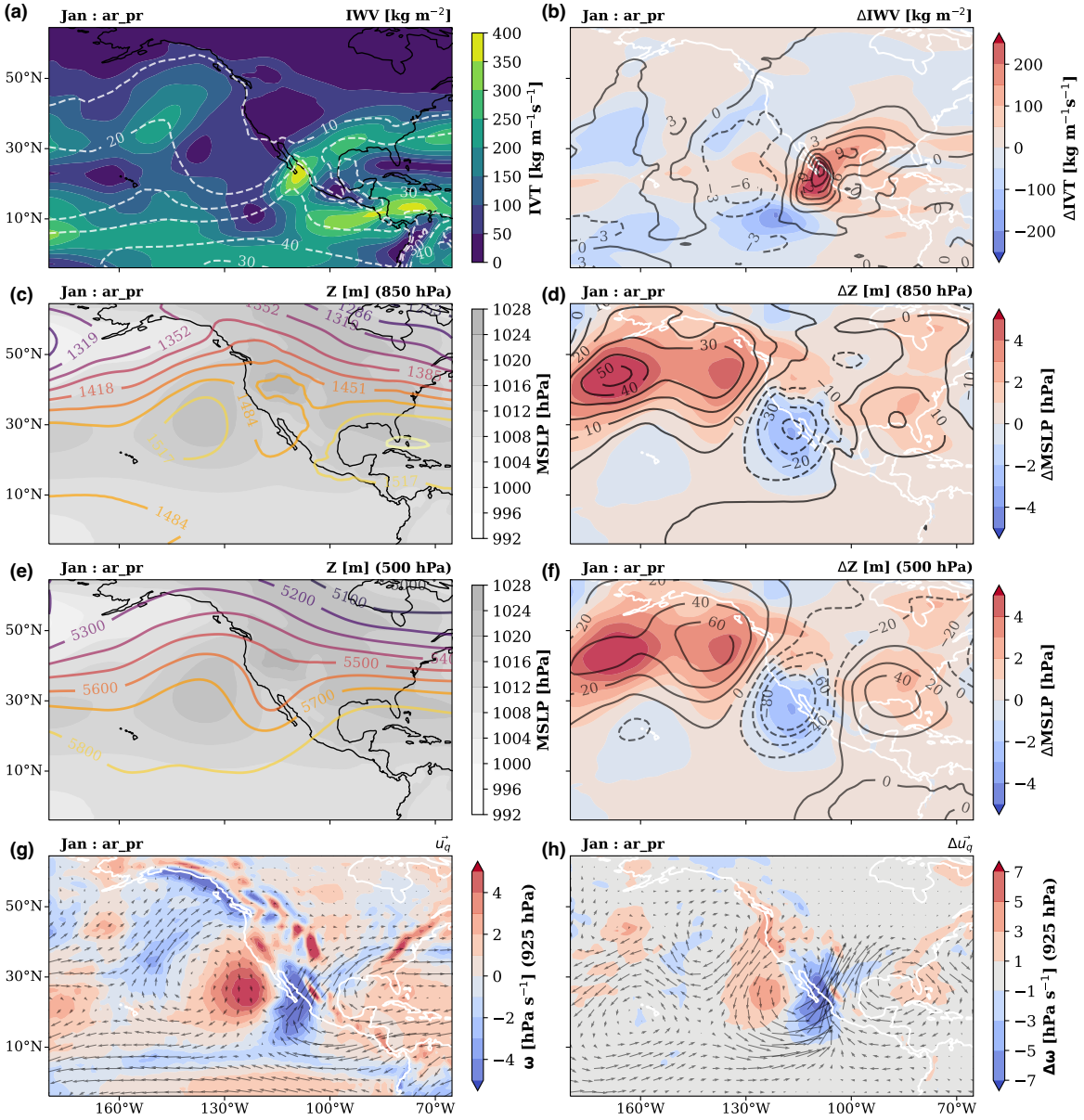

Figure S8. State of the atmosphere during AR landfalling and extreme precipitation at `Loc1` in January. Black contours variables are specified on the top-right of each plot. Left column: IWV, IVT, mean sea level pressure, geopotential height at 850 and 500 hPA, IVT direction (u_q), and ω at 650 hPa. Right column: anomalies with respect to the long-term mean for the same variables.

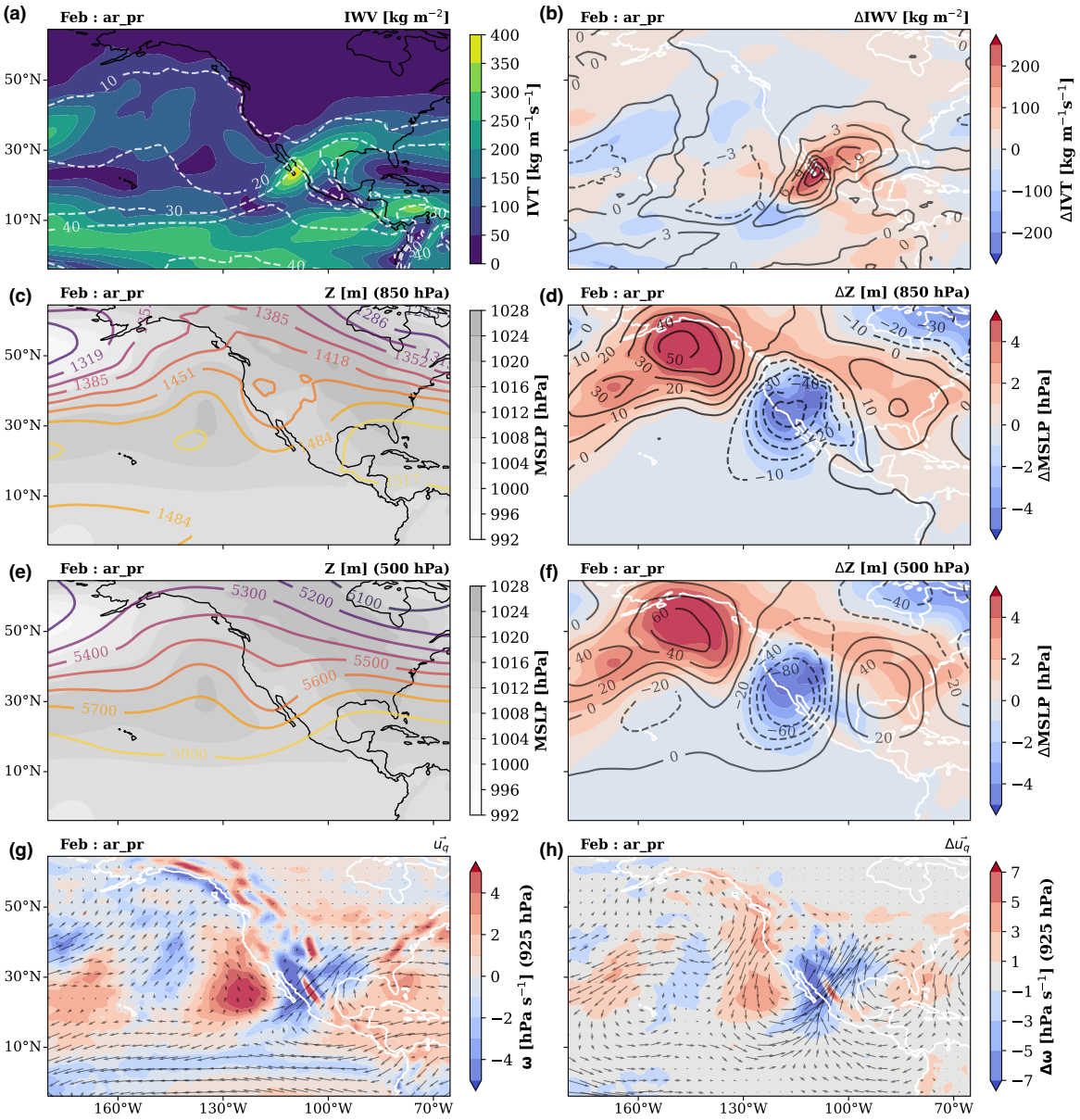

Figure S9. State of the atmosphere during AR landfalling and extreme precipitation at `Loc1` in February. Black contours variables are specified on the top-right of each plot. Left column: IWV, IVT, mean sea level pressure, geopotential height at 850 and 500 hPA, IVT direction (u_q), and ω at 650 hPa. Right column: anomalies with respect to the long-term mean for the same variables.

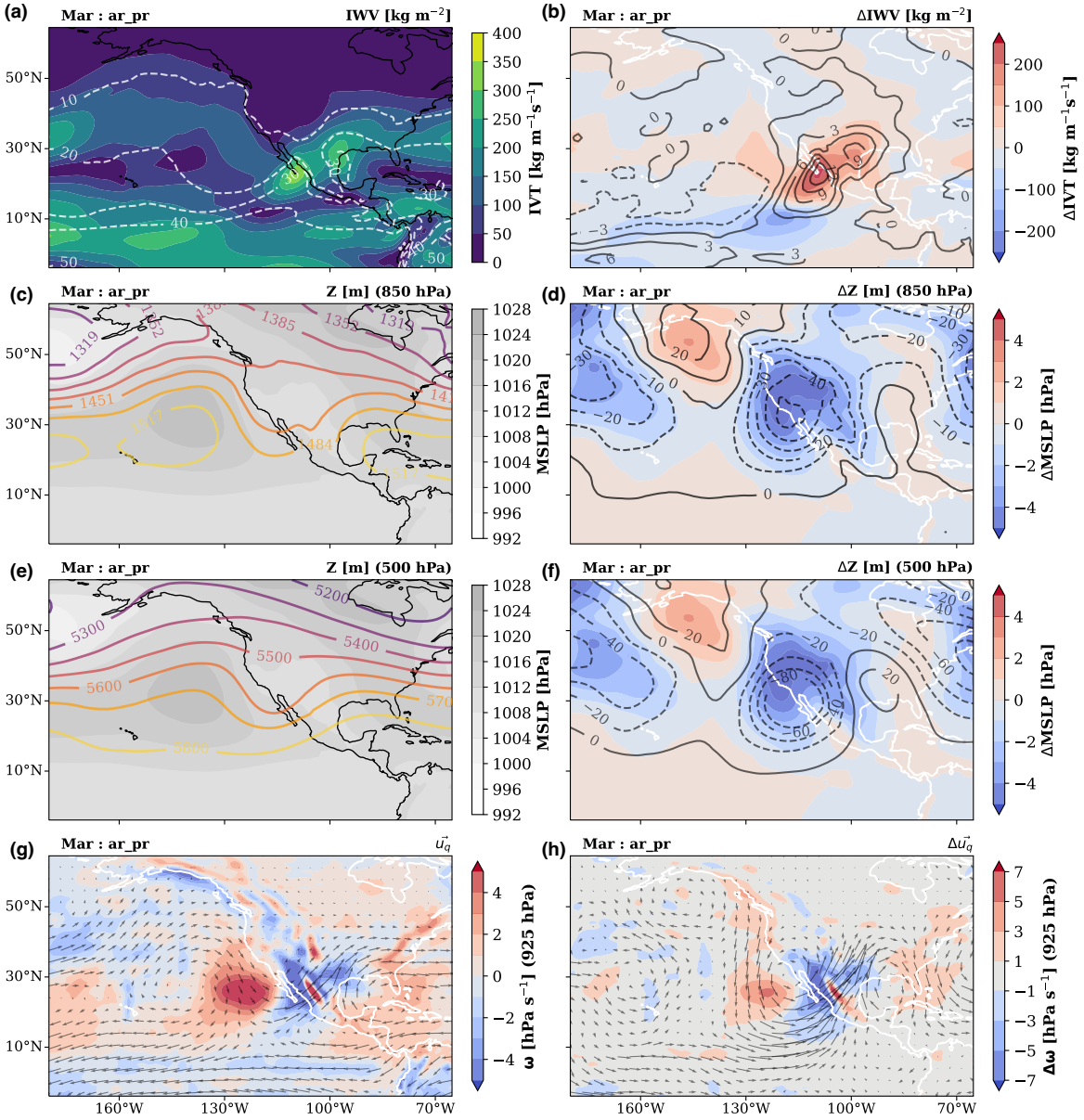

Figure S10. State of the atmosphere during AR landfalling and extreme precipitation at `Loc1` in March. Black contours variables are specified on the top-right of each plot. Left column: IWV, IVT, mean sea level pressure, geopotential height at 850 and 500 hPA, IVT direction (u_q), and ω at 650 hPa. Right column: anomalies with respect to the long-term mean for the same variables.

AR + Extreme Precipitation Composite at Loc2

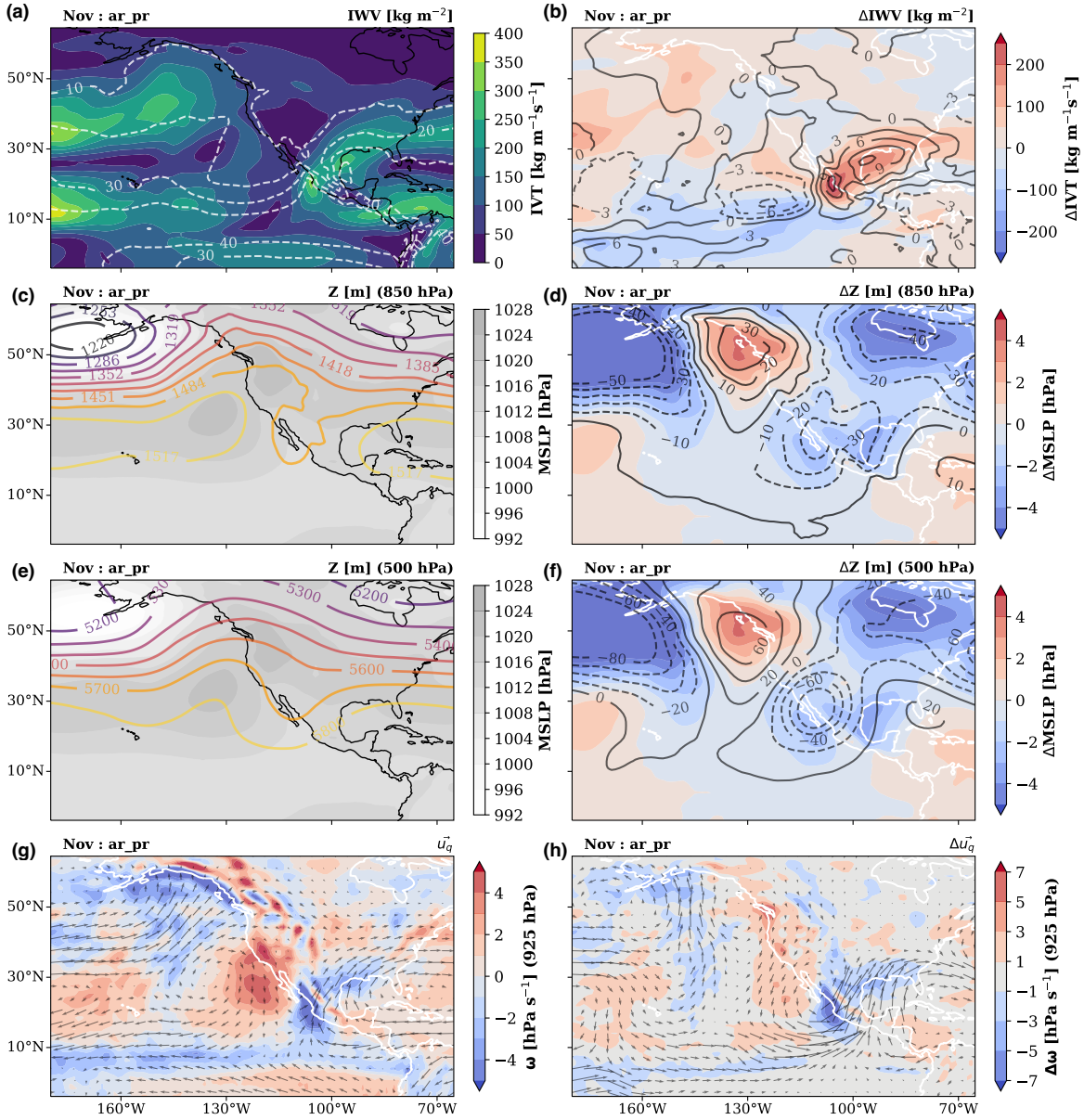

Figure S11. State of the atmosphere during AR landfalling and extreme precipitation at `Loc2` in November. Black contours variables are specified on the top-right of each plot. Left column: IWV, IVT, mean sea level pressure, geopotential height at 850 and 500 hPA, IVT direction (u_q), and ω at 650 hPa. Right column: anomalies with respect to the long-term mean for the same variables.

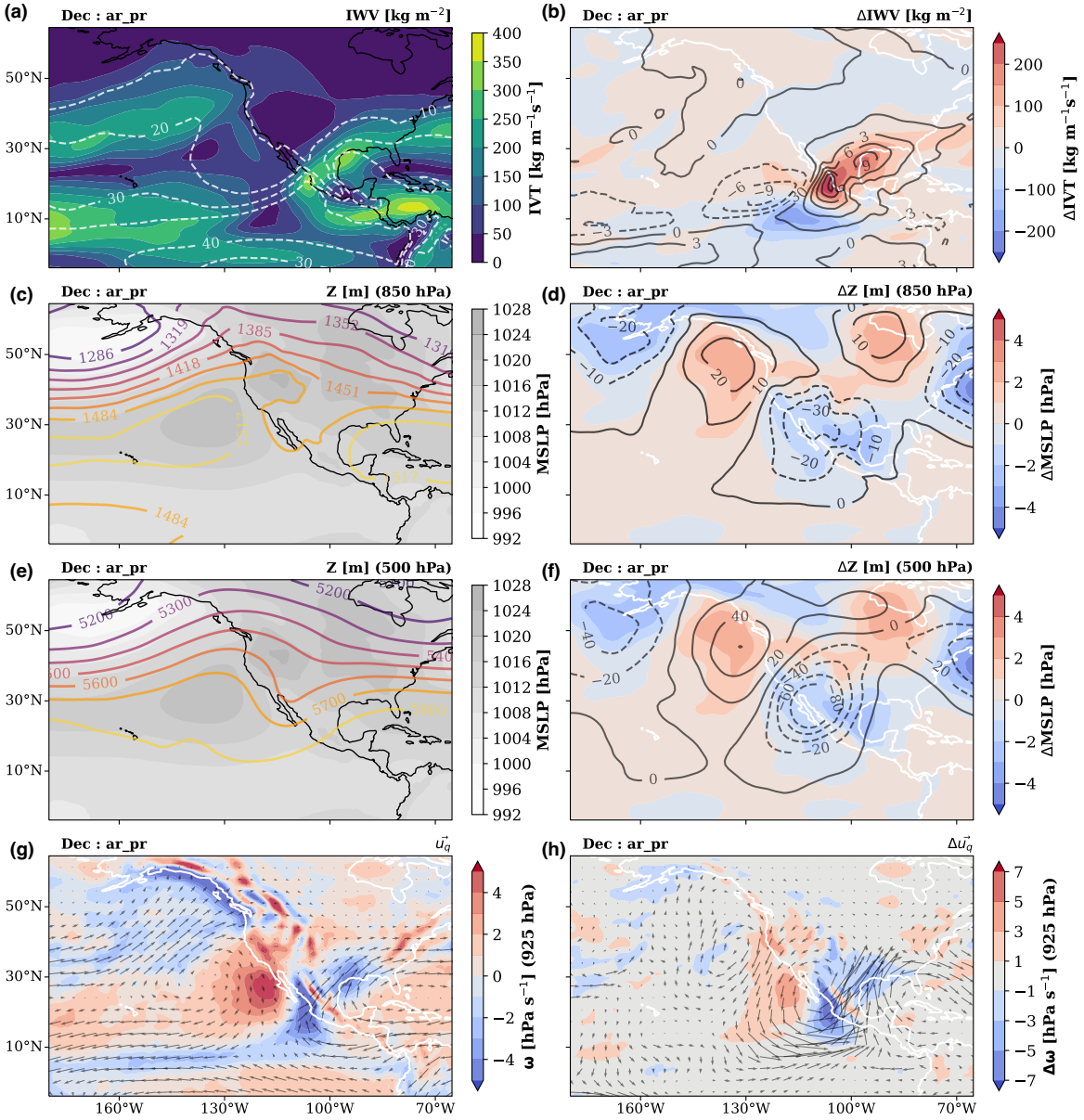

Figure S12. State of the atmosphere during AR landfalling and extreme precipitation at `Loc2` in December. Black contours variables are specified on the top-right of each plot. Left column: IWV, IVT, mean sea level pressure, geopotential height at 850 and 500 hPA, IVT direction (u_q), and ω at 650 hPa. Right column: anomalies with respect to the long-term mean for the same variables.

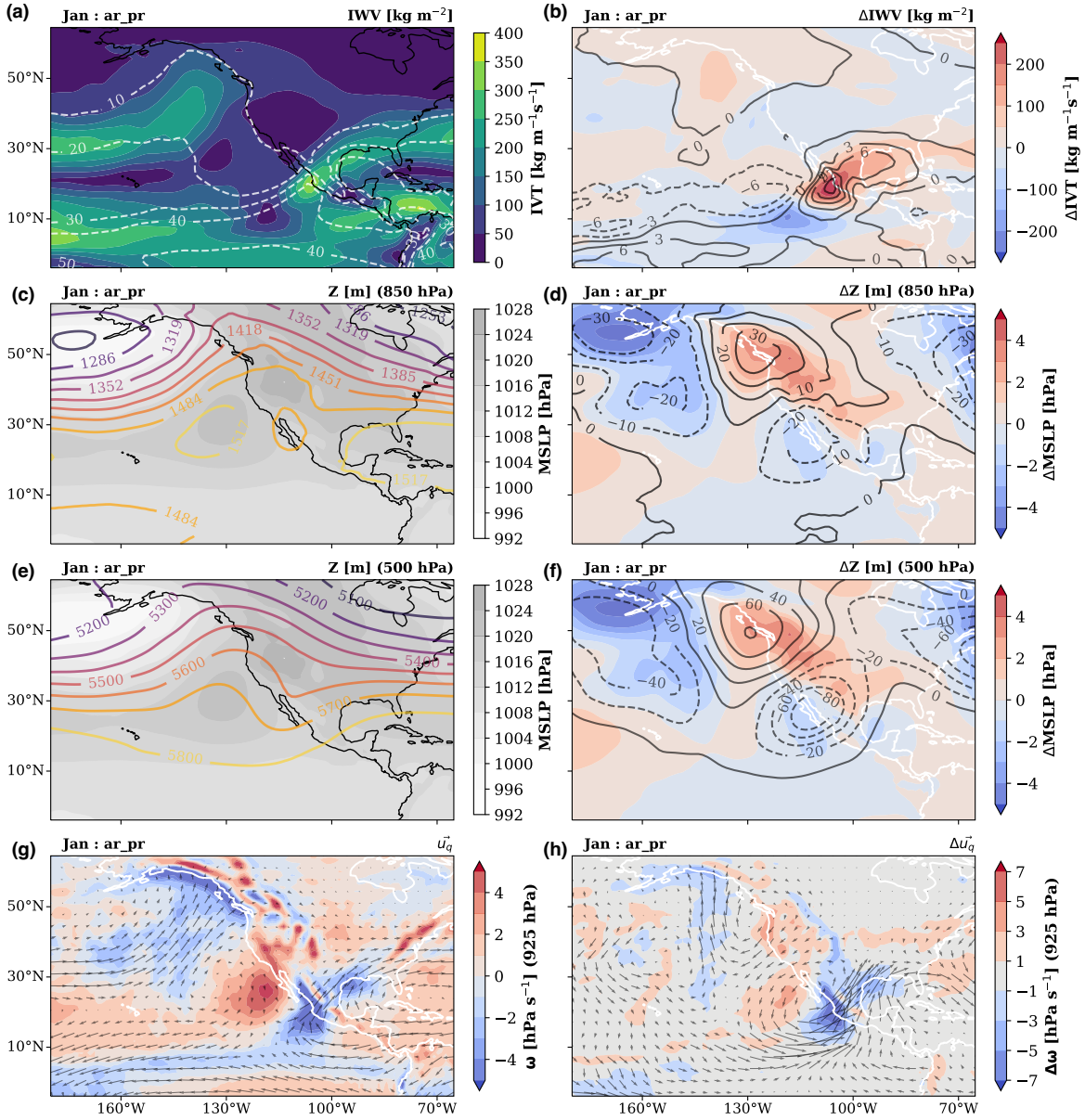

Figure S13. State of the atmosphere during AR landfalling and extreme precipitation at `Loc2` in January. Black contours variables are specified on the top-right of each plot. Left column: IWV, IVT, mean sea level pressure, geopotential height at 850 and 500 hPA, IVT direction (u_q), and ω at 650 hPa. Right column: anomalies with respect to the long-term mean for the same variables.

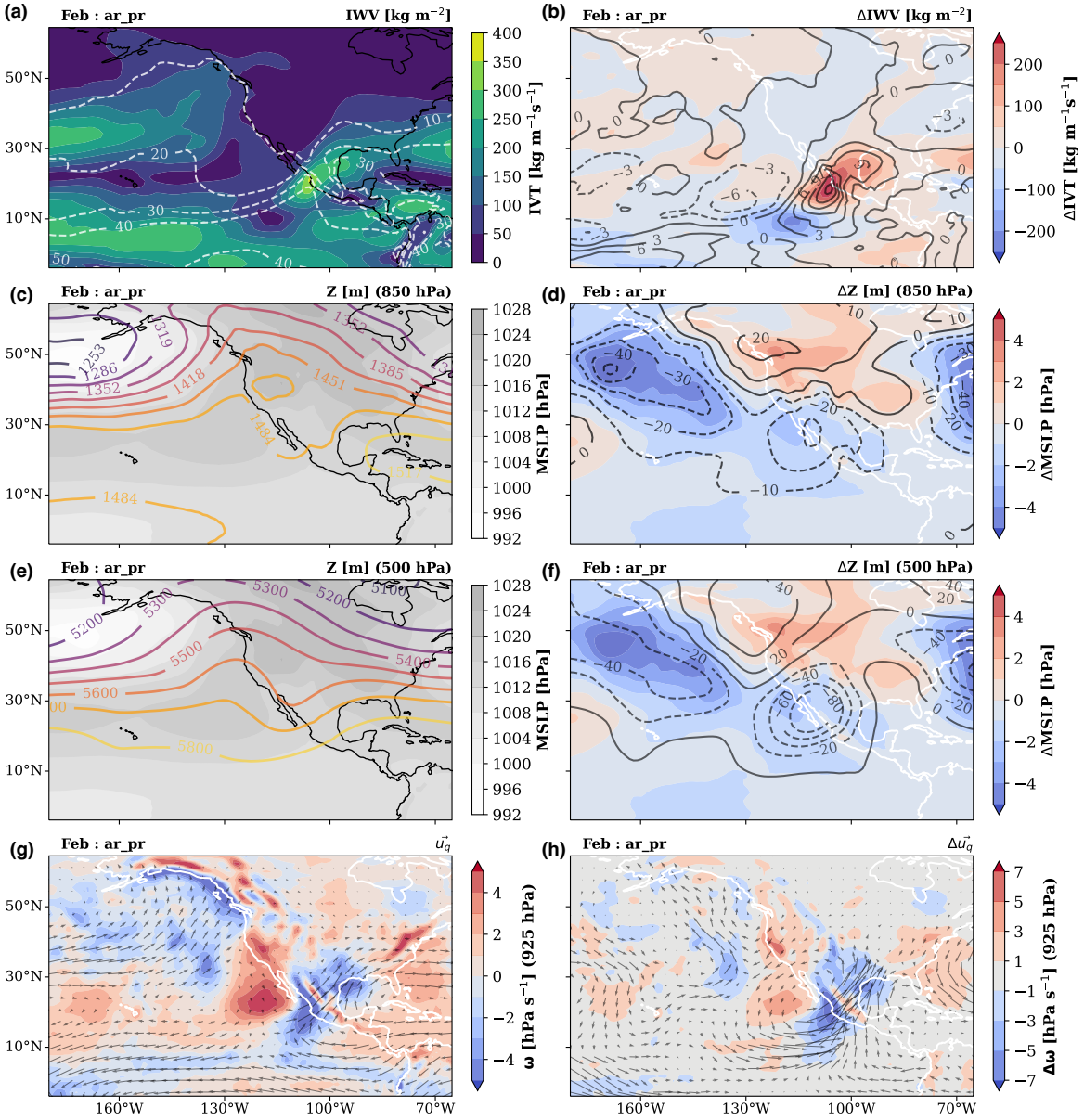

Figure S14. State of the atmosphere during AR landfalling and extreme precipitation at `Loc2` in February. Black contours variables are specified on the top-right of each plot. Left column: IWV, IVT, mean sea level pressure, geopotential height at 850 and 500 hPA, IVT direction (u_q), and ω at 650 hPa. Right column: anomalies with respect to the long-term mean for the same variables.

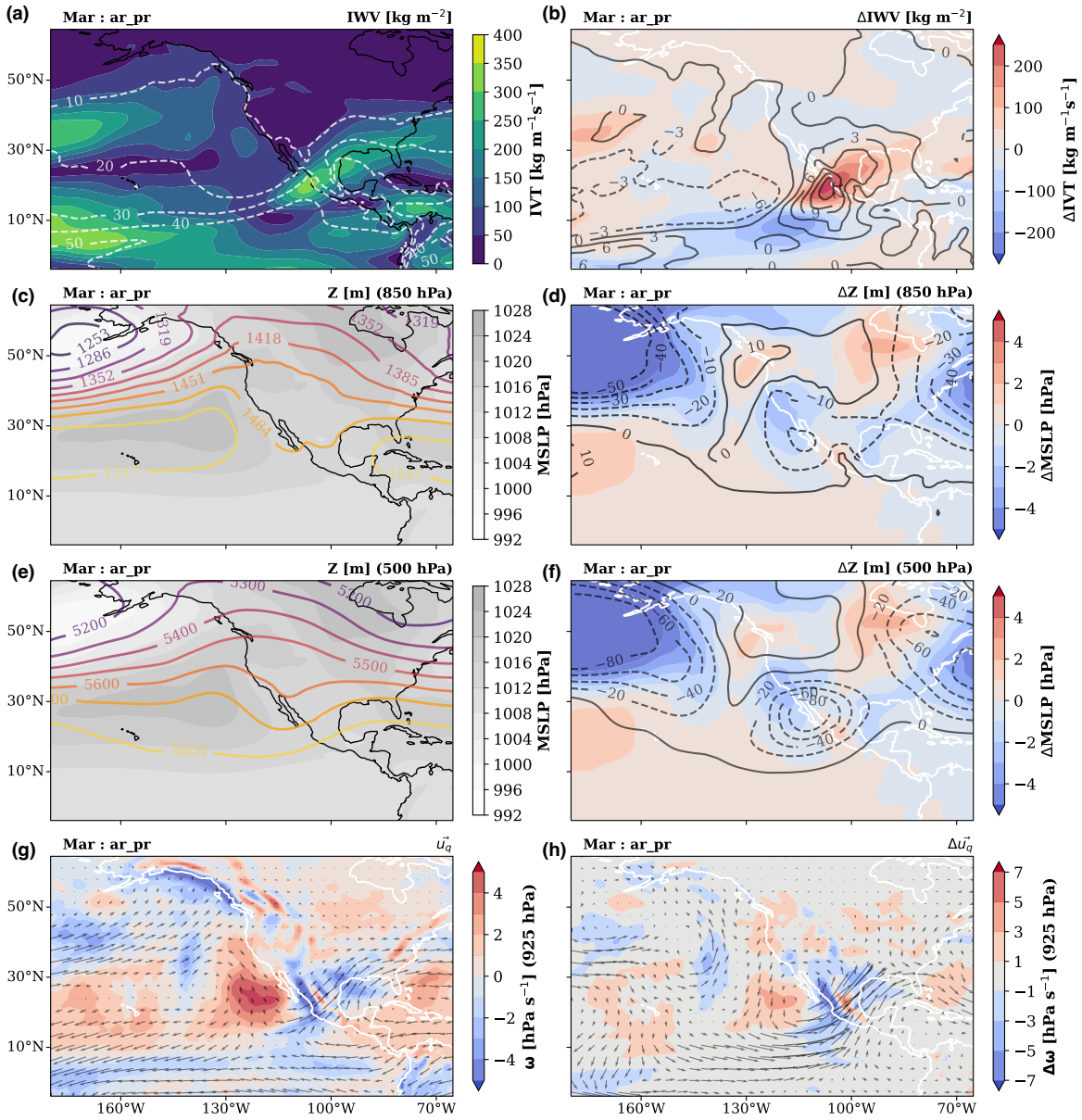

Figure S15. State of the atmosphere during AR landfalling and extreme precipitation at `Loc2` in March. Black contours variables are specified on the top-right of each plot. Left column: IWV, IVT, mean sea level pressure, geopotential height at 850 and 500 hPA, IVT direction (u_q), and ω at 650 hPa. Right column: anomalies with respect to the long-term mean for the same variables.

AR + No Precipitation Composite

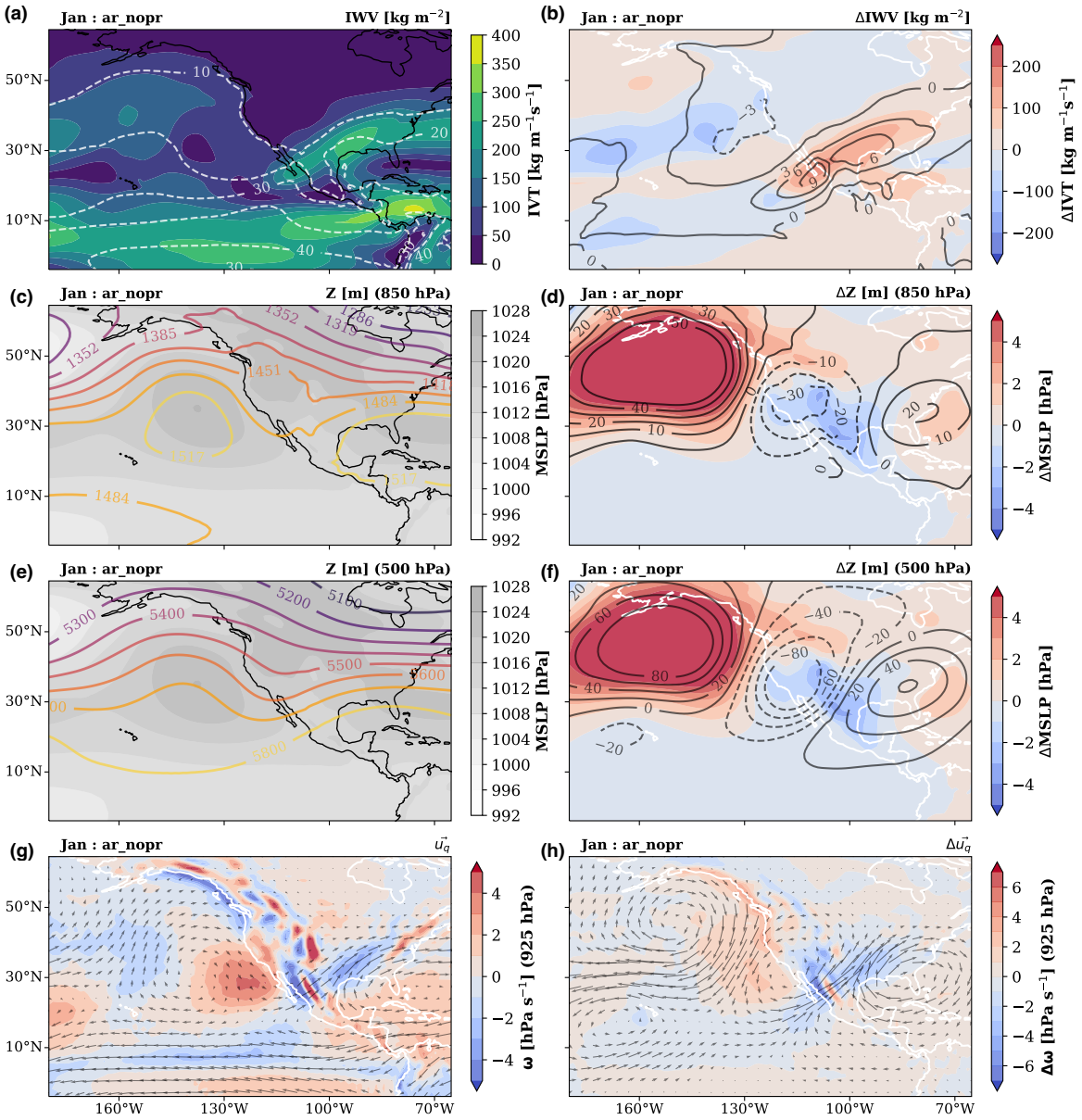

Figure S16. State of the atmosphere during AR landfalling and without extreme precipitation at `Loc1` in January. Black contours variables are specified on the top-right of each plot. Left column: IWV, IVT, mean sea level pressure, geopotential height at 850 and 500 hPA, IVT direction (u_q), and ω at 650 hPa. Right column: anomalies with respect to the long-term mean for the same variables.

Precipitation + no AR Composite

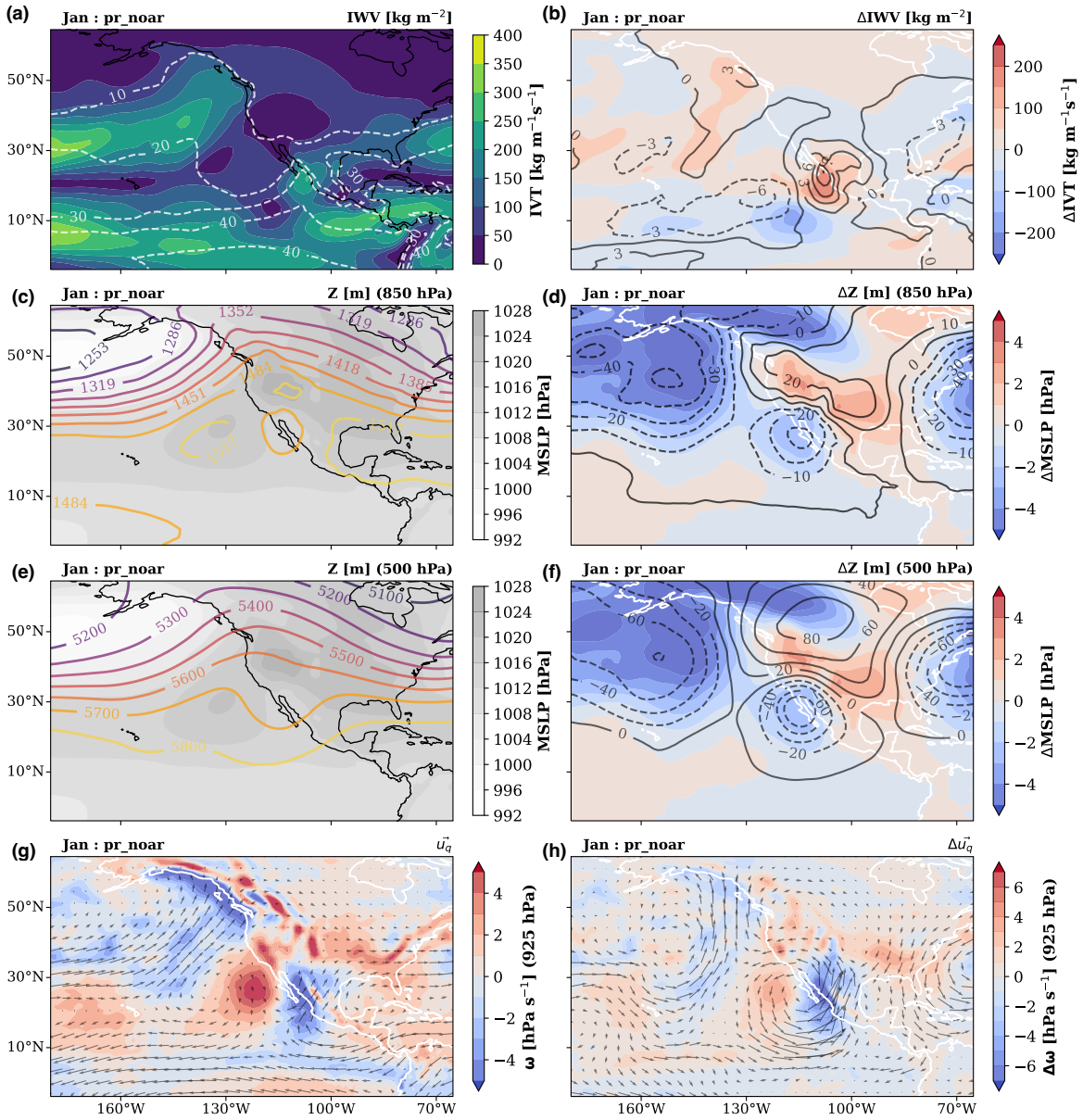

Figure S17. State of the atmosphere during extreme precipitation without AR landfalling conditions at `Loc1` in January. Black contours variables are specified on the top-right of each plot. Left column: IWV, IVT, mean sea level pressure, geopotential height at 850 and 500 hPA, IVT direction (u_q), and ω at 650 hPa. Right column: anomalies with respect to the long-term mean for the same variables.

Time Correlation between AR and Extreme Precipitation Events

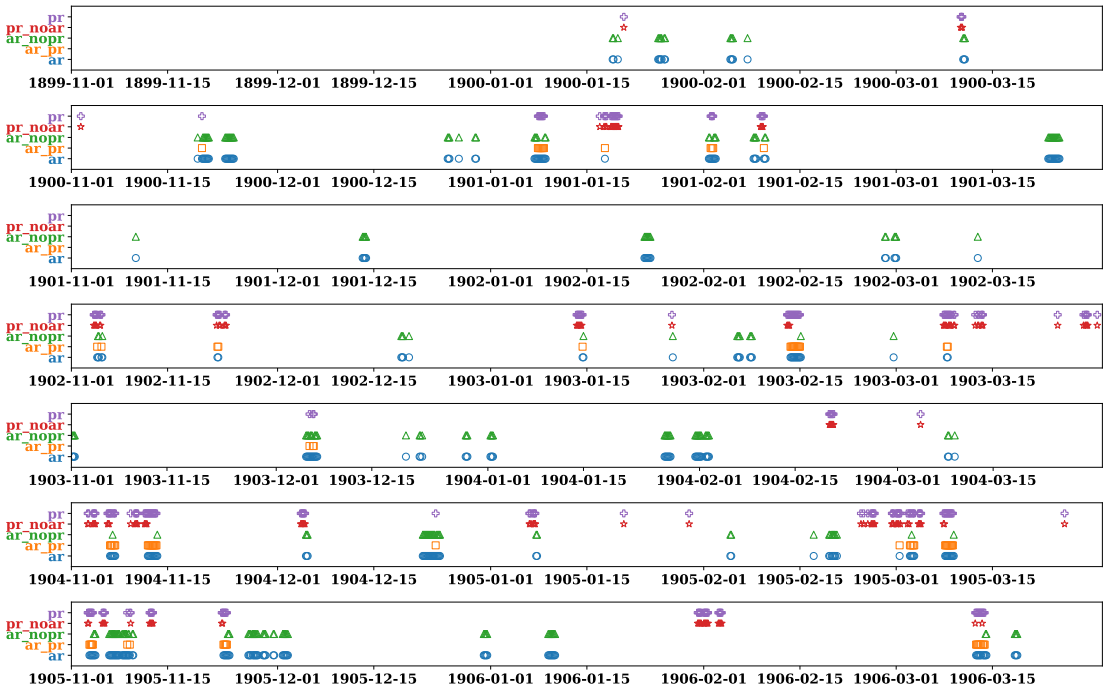

Figure S18. Time of event for each composite (*ar*, *ar_pr*, *ar_nopr*, *pr_noar*, and *pr*). Each subfigure shows a year in the 1900-2010 period to be able to clearly look at the overlap of events across composites. Blue circle markers represent *ar*, orange squares *ar_pr*, green triangles *ar_nopr*, red stars *pr_noar*, and purple crosses *pr*.

The same caption applies for Figures S19 through S25

Figure S19. Same caption as Figure S18

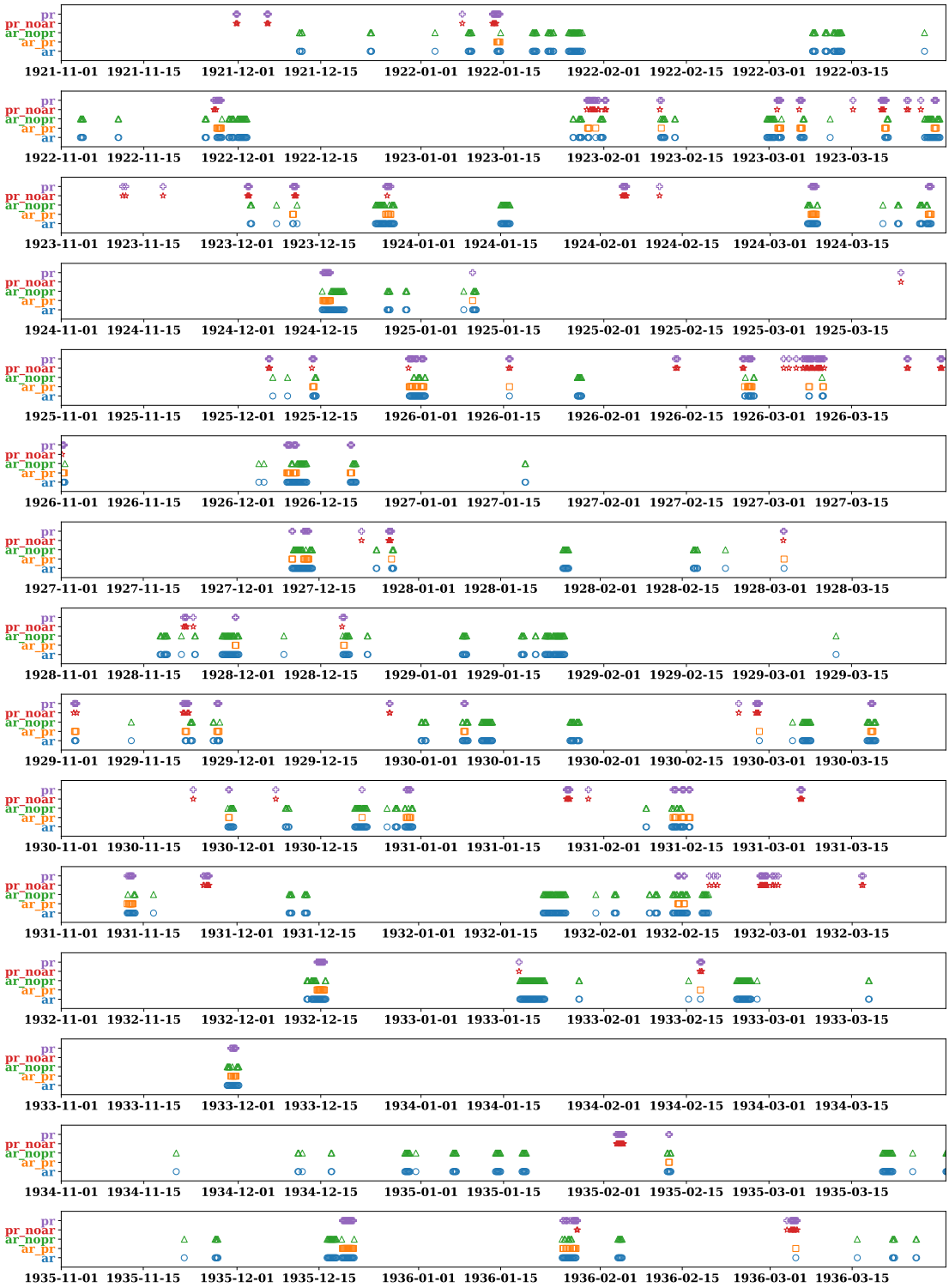

Figure S20. Same caption as Figure S18

Figure S21. Same caption as Figure S18

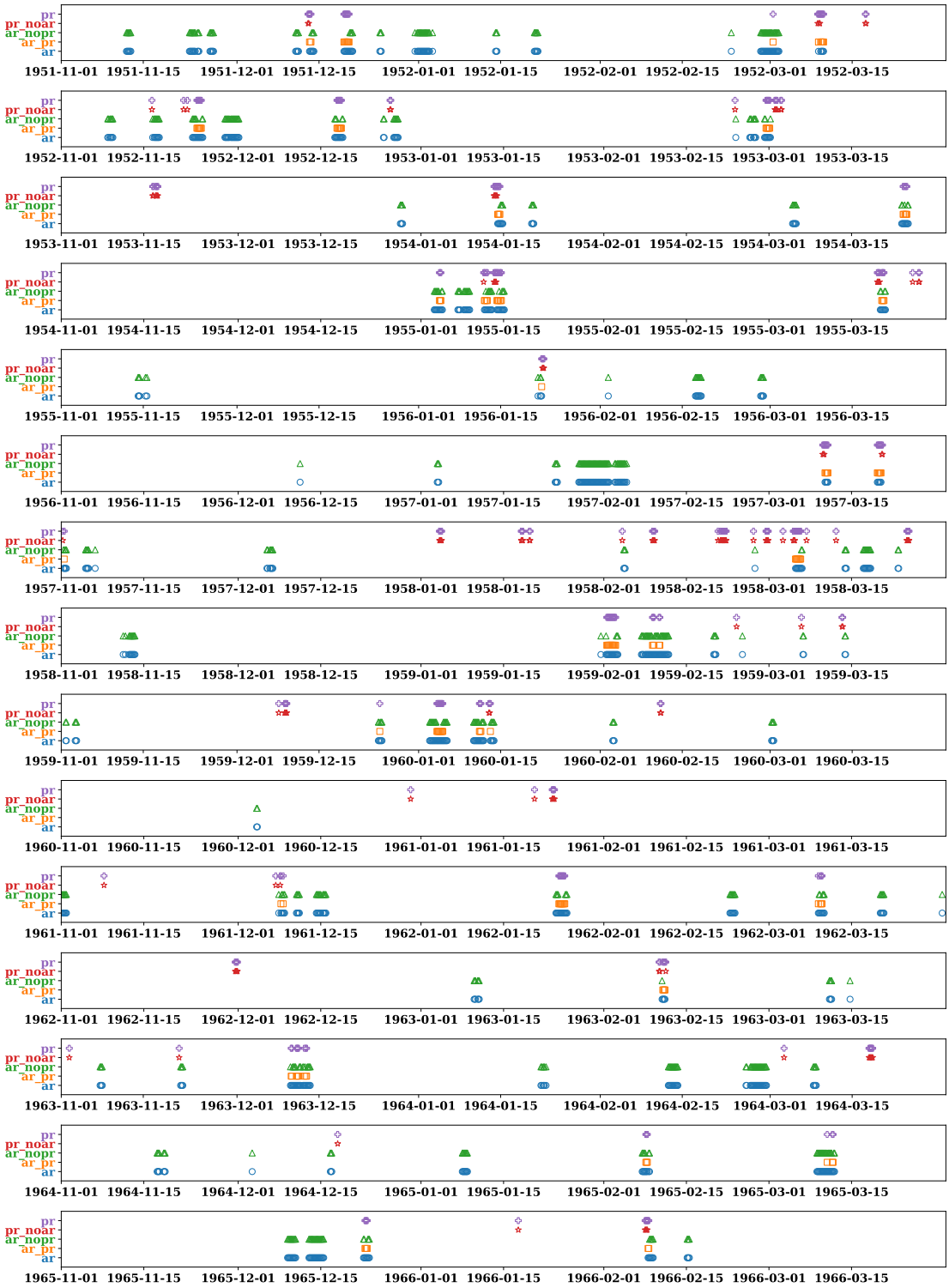

Figure S22. Same caption as Figure S18

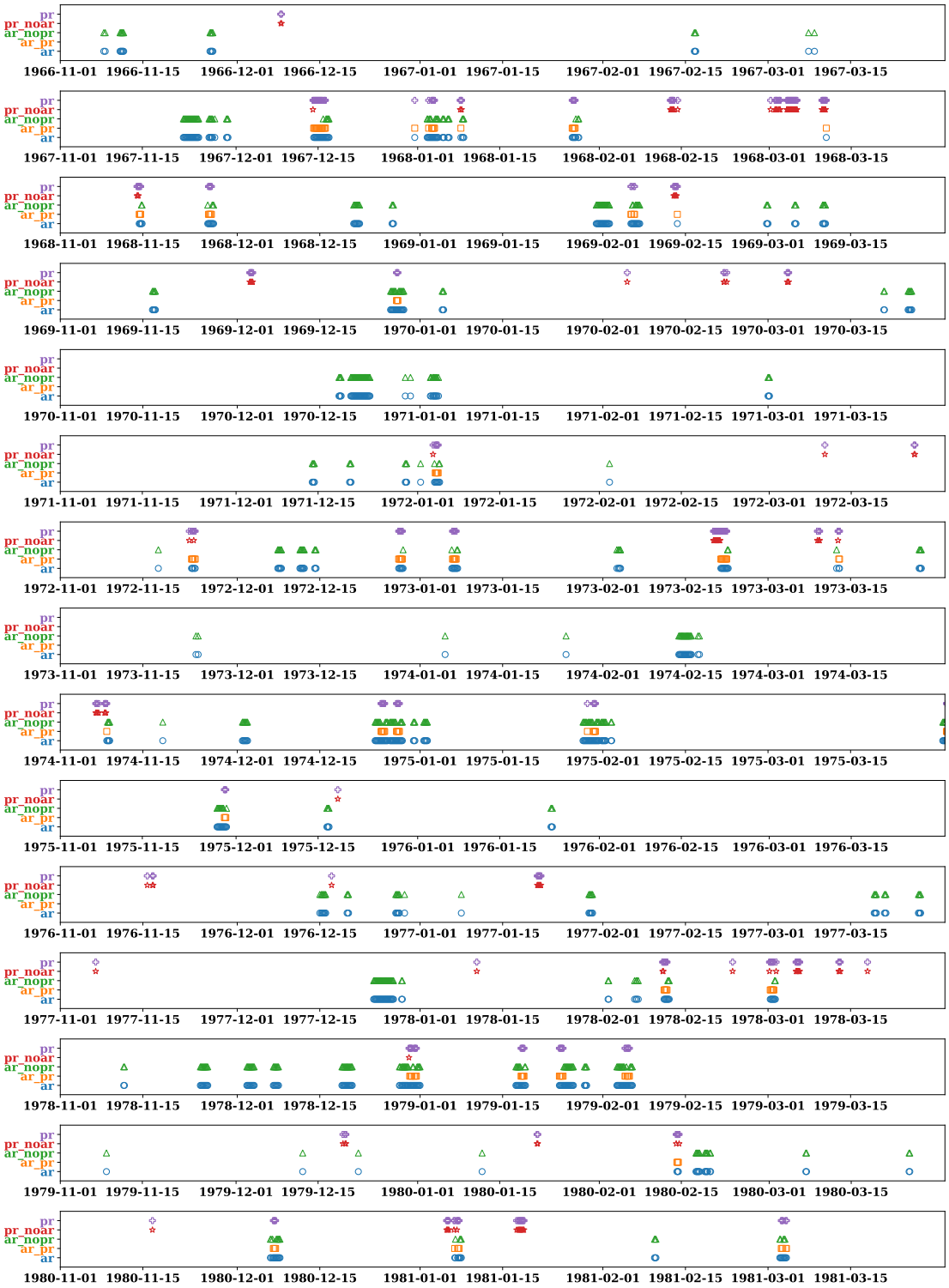

Figure S23. Same caption as Figure S18

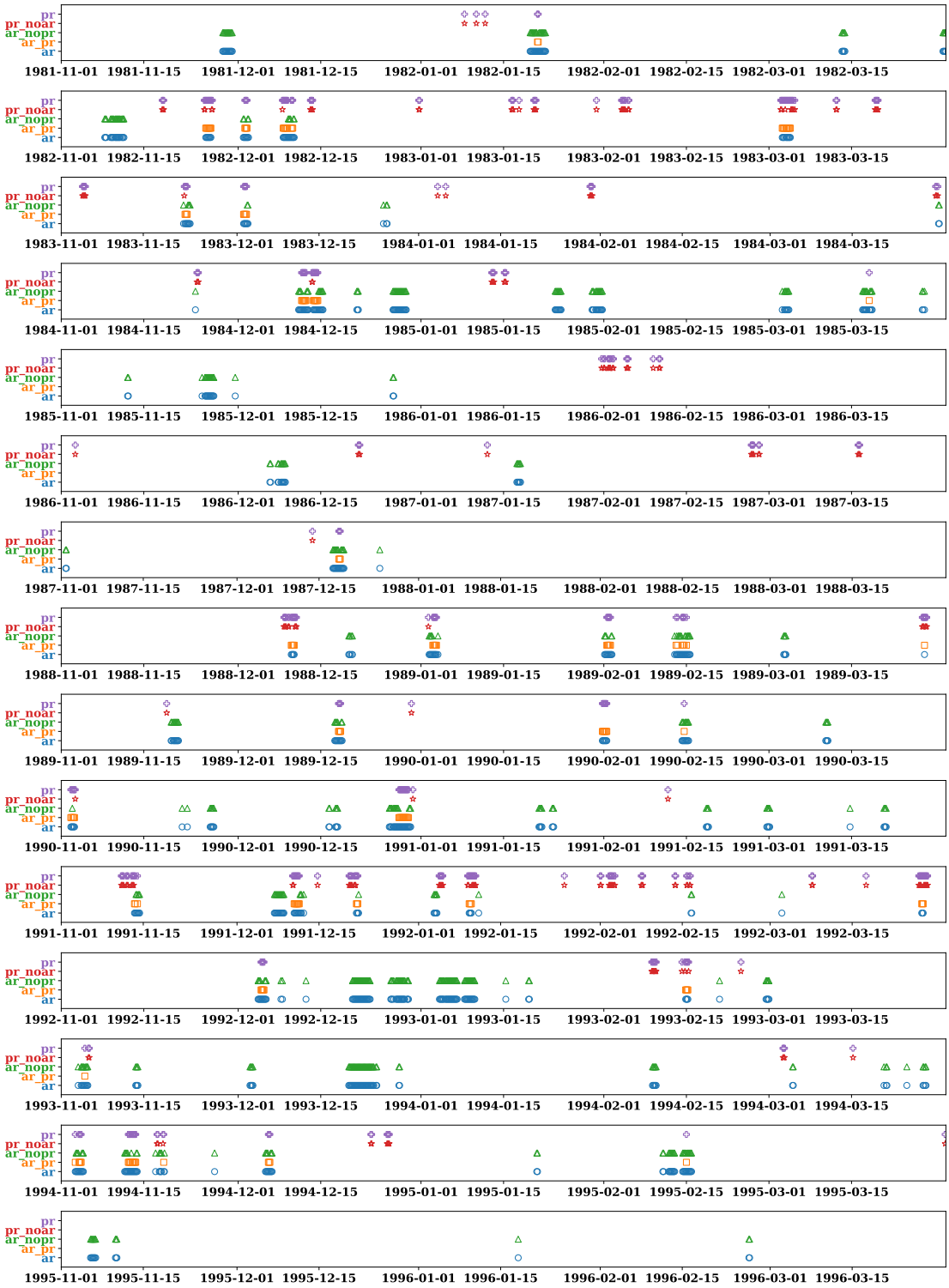

Figure S24. Same caption as Figure S18

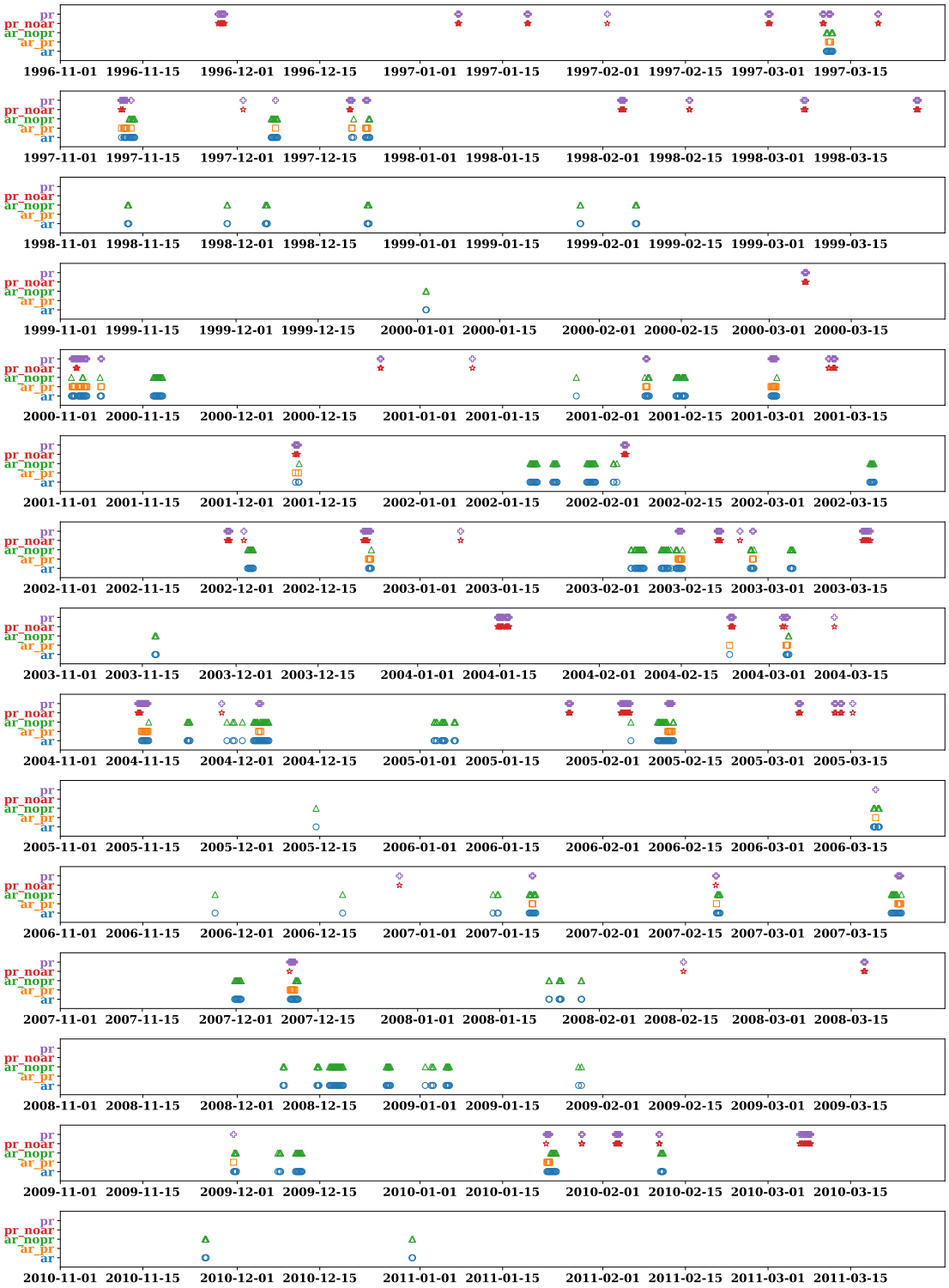

Figure S25. Same caption as Figure S18